Supporting Information

Synergistic Regulation of Bidirectional Conversion of LiPSs and Li_2S Using Anthraquinone as a Redox Mediator

Huijuan You[a,1], Zining Wang[b,1], Xuyun Wang[a,*], Jianwei Ren[c,*], HuiWang[a], Rongfang Wang[a**]

[a] College of Chemical Engineering, Qingdao University of Science and Technology, Qingdao, 266042, China

[b] School of Chemical Science and Engineer, Tongji University, 1239 Siping Road, Shanghai 200092, China

[c] Department of Chemical Engineering, University of Pretoria, cnr Lynnwood Road and Roper Street, Hatfield 0028, South Africa

***Corresponding author.**

E-mail address: wangxy@qust.edu.cn (X. Wang); rfwang@qust.edu.cn (R. Wang); jianwei.ren@up.ac.za (J. Ren)

[1] H. Y. and Z. W. contributed equally to this paper.

Preparation of Co-N-C sample

In a typical process, 1 g of peptone and 0.03 mmol of $Co(NO_3)_2 \cdot 6H_2O$ were dissolved together in 2 mL of deionized water and the mixture was ultrasonicated for 5−10 min until fully dissolved. The solution was then frozen for 12 h in forming ice blocks, which were subsequently freeze-dried for 12 h. The dried material was combined with NaCl (10 g) and subjected to a ball milling operation at 550 rpm for 3 h. The milled mixture was transferred to a tube furnace, which was heated up gradually to 900 °C at a rate of 5 °C/min under an N_2 atmosphere, and maintained at this temperature for 1 h for high-temperature pyrolysis. After cooling, the final

product was collected and washed to remove residues before drying in an oven at 60 °C.

Preparation of AQ/Co-N-C sample

Typically, Co-N-C (60 mg) was dispersed in a 0.05 mM AQ solution (20 mL) and the mixture was stirred for 30 min using a magnetic stirrer. The product was then centrifuged, and dried in an oven at 60 °C for 6 h.

Preparation of S@Co-N-C and S@AQ/Co-N-C samples

The Co-N-C and AQ/Co-N-C samples prepared in *Steps Preparation of Co-N-C sample* and *Preparation of Co-N-C sample*, respectively, were each individually mixed with sublimed sulfur at a mass ratio of 2:3. The mixture underwent grilling for 30 min before being transferred into a reactor within an argon-filled glove box. The reactor was subsequently placed in a pre-heated oven at 155 °C for 12 h to produce the S@Co-N-C and S@AQ/Co-N-C samples.

Preparation of Li_2S_6 solutions

Li_2S and sublimed sulfur were combined in a molar ratio of 1:5 and added to a mixed solvent of ethylene glycol dimethyl ether and 1,3-dioxolane (DME/DOL, v/v = 1:1). The mixture was heated up to 60 °C and stirred for 24 h to yield the 0.2 M Li_2S_6 solution. Similarly, a 5 mM Li_2S_6 solution was prepared using the same procedure.

Adsorption Experiments

In a typical experiment, 5 mg of Co-N-C and AQ/Co-N-C samples were separately added to a 5 mM Li_2S_6 solution (5 mL). The mixtures were allowed to stand for 2 h to observe any color changes.

Physical Characterization

In-situ synchrotron radiation measurements were performed at the Shanghai Synchrotron Radiation Facility using the BL08U1A beamline. X-ray Powder Diffraction (XRD) analysis was performed on an X-ray diffractometer (Rigaku MiniFlex 600, Japan) with a scanning rate of 10 °/min across a 2θ range of 10–80°. Transmission Electron Microscopy (TEM) was performed using a JEOL JEM-2000FX transmission electron microscope (Japan), also with imaging across different regions. Scanning Electron Microscopy (SEM) imaging was conducted with a Carl Zeiss Ultra Plus scanning electron microscope (Germany), capturing various regions of the sample. UV-Vis Spectroscopy measurements were obtained with a UV-5800 PC UV-visible spectrophotometer, covering a wavelength range from 200 to 400 nm.

Evaluation of Electrochemical Performance

Typically, S@AQ/Co-N-C, conductive carbon black Super P, and binder PVDF in a mass ratio of 7:2:1 was dissolved in NMP under continuous stirring. The resulting slurry was then coated onto an aluminum foil current collector and dried for 12 h at 60 °C to form the sulfur cathode. The assembling process of coin cell was carried out in an argon-filled glove box, using the 1.0 M LiTFSI solution in DME/DOL (volume ratio = 1:1) with 1.0% $LiNO_3$ as the electrolyte, Celgard 2400 (diameter: 16 mm) as the separator, metallic lithium (diameter: 15.6 mm, thickness: 0.45 mm) as the anode, and a CR2032 stainless steel battery casing. Unless otherwise noted, the mass loading of sulfur in the electrode was approximately 1.2–1.4 mg cm^{-2} (diameter: 12 mm), and the electrolyte-to-sulfur (E/S) ratio was about 40 μL mg^{-1}. For the symmetric cell, the ingredients of AQ/Co-N-C, PVDF, and Super P in a mass ratio of 8:1:1 were mixed and dissolved in NMP, and the obtained slurry was coated onto carbon paper, which was then dried at 60 °C. In assembling the symmetric cell, A 0.2 M Li_2S_6 solution (60 μL) was used as the electrolyte.

The discharge and constant current charge tests were carried out on a Newway battery system, and the voltage range was set between 1.7 and 2.8 V. The

electrochemical impedance spectroscopy (EIS) measurements and cyclic voltammetry (CV) were done on an electrochemical analyzer (CHI 650D). The EIS tests covered the frequency range of 100 kHz−10 mHz. All those experiments were conducted at room temperature. For the CV measurements, a scanning rate of 0.1 mV s^{-1} was applied within the voltage window of 1.7 to 2.8 V. The peak current observed at scanning rates between 0.1 and 0.5 mV s^{-1} was analyzed using the Randles-Sevcik equation.

$$I_{\mathrm{P}} = (2.69 \times 10^5) \times n^{1.5} \times A \times D_{\mathrm{Li}}^{0.5} \times C_{\mathrm{Li}} \times v^{0.5}$$

In this equation I_{P} represents the peak current (A), n denotes the number of electrons involved in the reaction (n=2), A represents the electrode area, D_{Li} is the diffusion coefficient of Li^+, C_{Li} represents the concentration of Li^+ in the electrolyte, and v denotes the potential scan rate.

Theoretical Calculation

Calculations were conducted using the B3LYP density functional method in the Gaussian 09 program, with the 6-31G(D) basis set. Dispersion corrections were applied using the empirical keyword (em=gd3bj). All molecular structures were optimized and confirmed to have no imaginary frequencies. The lowest unoccupied molecular orbital (LUMO), highest occupied molecular orbital (HOMO), and electrostatic surface potential (ESP) were computed and visualized using Multiwfn and Visual Molecular Dynamics (VMD).

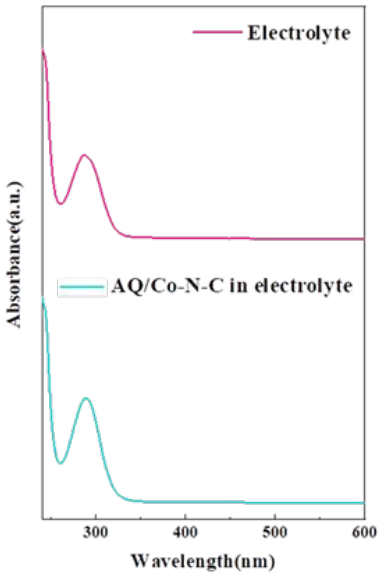

Figure S1. UV-Vis spectra of the pure electrolyte and the electrolyte with dispersed AQ/Co-N-C sample.

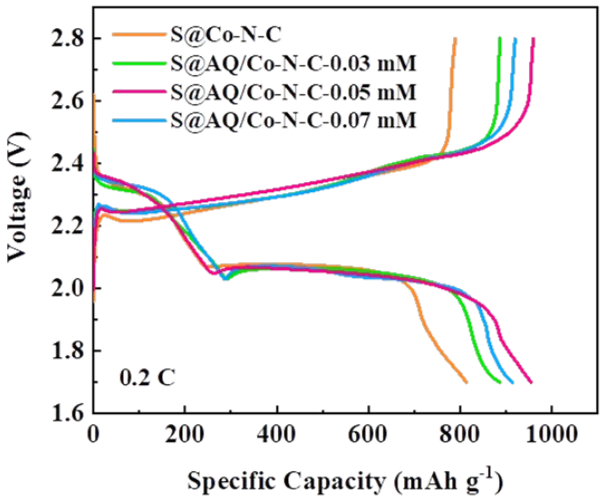

Figure S2. Charge and discharge curves of S@Co-N-C and S@AQ/Co-N-C samples at different concentrations at 0.2 C.

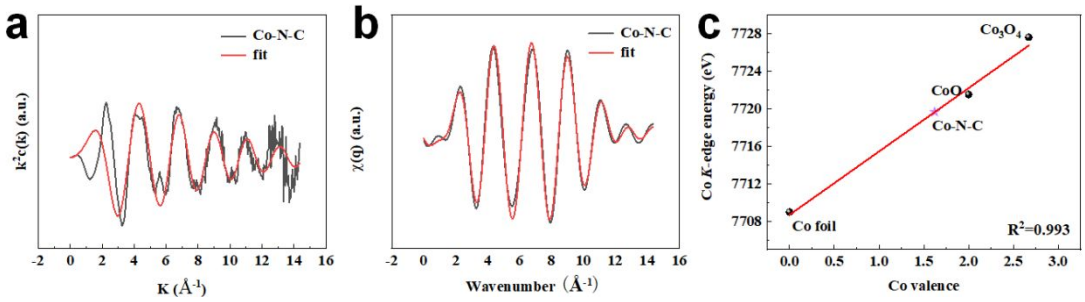

Figure S3. (a) K-space oscillation fitting of Co-N-C, (b) Q-space oscillation fitting of Co-N-C, (c) Linear fitting curve of Co-N-C cathodes and reference samples derived from the corresponding Co K-edge XANES spectra.

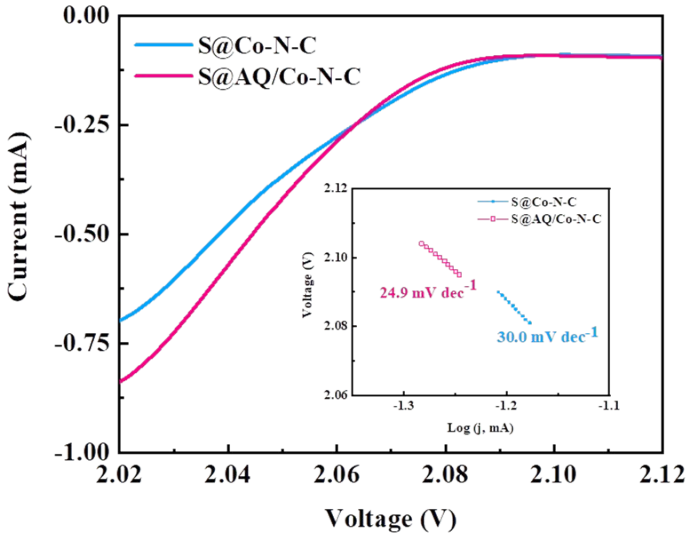

Figure S4. Linear voltammetry curves and corresponding Tafel slopes for the reduction processes of S@Co-N-C and S@AQ/Co-N-C samples.

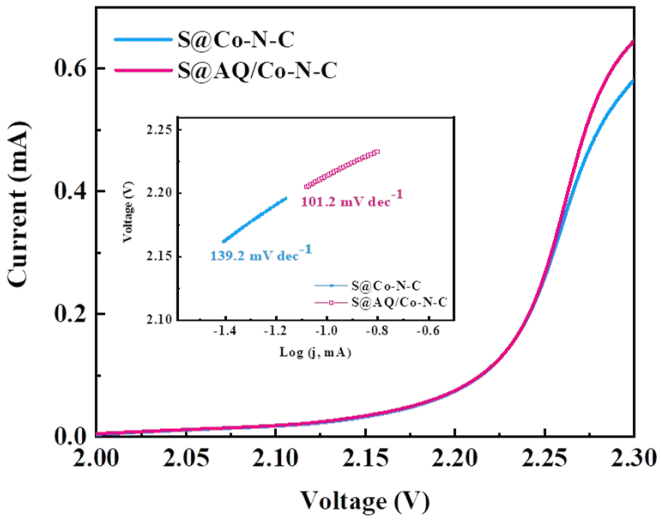

Figure S5. Linear voltammetry curves and corresponding Tafel slopes for the oxidation processes of S@Co-N-C and S@AQ/Co-N-C samples.

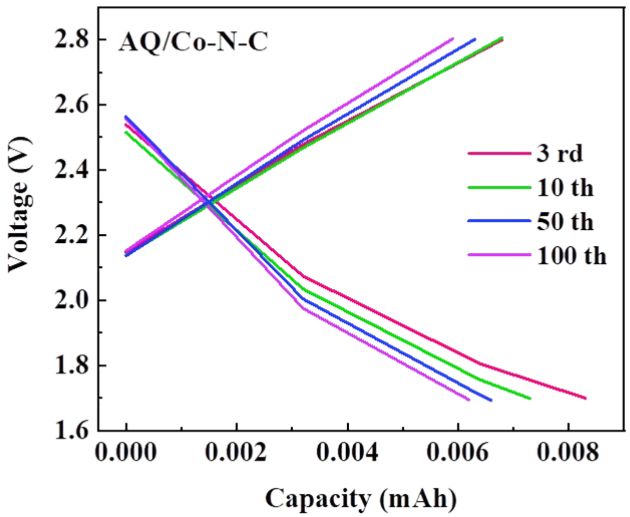

Figure S6. Charge and discharge curves of the AQ/Co-N-C sulfur-free carbon cathode sample.

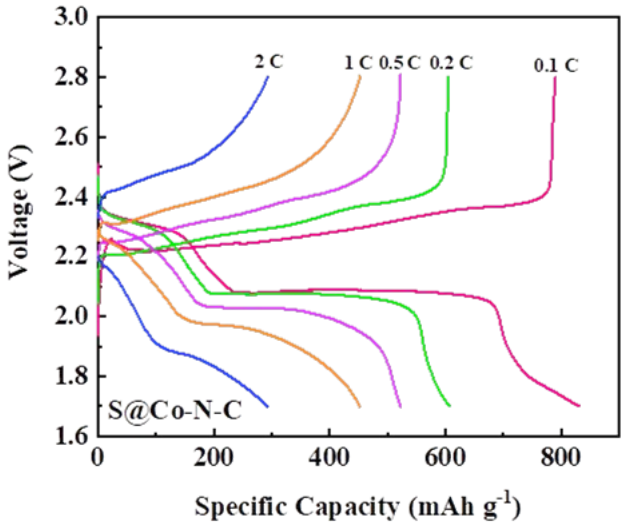

Figure S7. Charge and discharge curves of S@Co-N-C sample at different current densities.

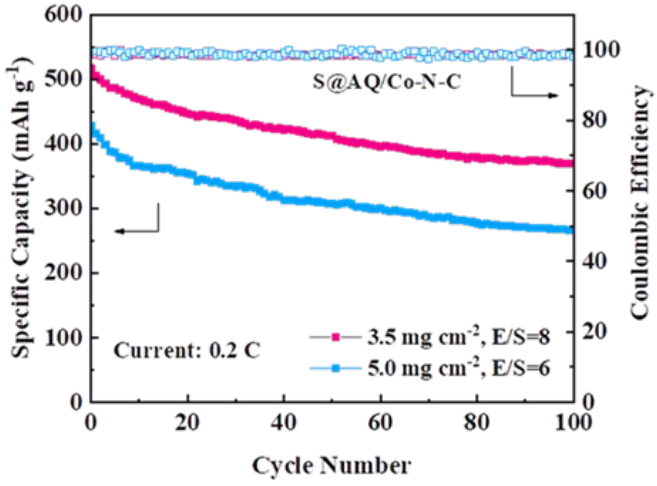

Figure S8. Cycling stability of the S@AQ/Co-N-C sample at sulfur loadings of 3.5 mg cm^{-2} (E/S ratio: 8 μL mg^{-1}) and 5.0 mg cm^{-2} (E/S ratio: 6 μL mg^{-1}) under 0.2 C.

Table S1. Structural parameters of the Co-N-C catalysts extracted from the EXAFS fitting.

Sample	Scattering pair	Coordination number	Bond length R(Å)	R factor (100%)
Co-N-C	Co-N	3.75	1.84	0.020

Table S2. Li^+ diffusion coefficients of the S@Co-N-C and S@AQ/Co-N-C samples.

D_{Li^+} ($cm^2\ s^{-1}$)	**A (cathodic peak) S_8→LiPSs (Li_2S_x, 4≤x≤8)**	**B (cathodic peak) LiPSs (Li_2S_x, 2≤x<4) →Li_2S_2/Li_2S**	**C (anodic peak) Li_2S_2/Li_2S→LiPSs→S_8**
S@Co-N-C	$3.73*10^{-9}$	$5.87*10^{-9}$	$9.48*10^{-9}$
S@AQ/Co-N-C	$4.25*10^{-9}$	$6.61*10^{-9}$	$1.12*10^{-8}$

Table S3. Performance comparison with other electrodes reported in literature.

Material type	**Initial capacity ($mAh\ g^{-1}$)**	**High rate capacity ($mAh\ g^{-1}$)**	**Capacity decay rate per cycle**	**Ref.**
PG-DAAQ	1198/0.1 C	899/1 C	0.143%/1 C/200	[1]
MB-AQ/rGO/S	1291/0.1 C	884/1 C	0.005%/1 C/700	[2]
S@DMAQ/C	1071/0.1 C	637/1 C	0.038%/1 C/600	[3]
S/N-PCS	1035/0.1 C	755/1 C	0.047%/1 C/650	[4]
Fe_3O_4/FeP@C─S	1402/0.1 C	1093/1 C	0.126%/1 C/300	[5]
Ni@NCNT	1527/0.1 C	1035/1 C	0.060%/1 C/500	[6]
Li_2S/PDSe	880/0.1 C	790/0.5 C	0.025%/0.5 C/200	[7]
CC@CoSNC/$CoCp_2$−S	1540/0.1 C	904/0.5 C	0.053%/0.5 C/300	[8]
Co_7Mo_3B/S	1446.2/0.1 C	1324.9 /1 C	0.065%/1 C/400	[9]
S/NQ-rGO	1254/0.1 C	1204/1 C	0.089%/1 C/500	[10]
APC/S	744/0.16 C	1016/0.5 C	0.035%/0.5 C/800	[11]
S@AQ/Co-N-C	1290/0.1 C	570/1 C	0.060%/1 C/600	This work

References

[1] Lai, T.; Manthiram, A. Phloroglucinol–2,6-Diaminoanthraquinone as a Durable Redox Mediator for Enhancing Conversion Reaction Kinetics in Lithium-Sulfur Batteries. Adv. Funct. Mater. 2024, 2405814-2405822.

[2] Zheng, Q.; Fan, X.; Liu, G.; Hou, Q.; Fan, J.; Zheng, M.; Dong, Q. Enhancing sulfur cathode process via a functionalized complex molecule. Nano Res. 2022, 16 (6), 8385-8393.

[3] Gao, R.; Ji, S.; Wang, K.; Linkov, V.; Ma, X.; Wang, H. 2,6-dimethoxy anthraquinone as redox mediator for the reversible deposition-dissolution of Li_2S in lithium-sulfur batteries. Chem. Eng. J. 2024, 484, 149611-149620.

[4] Pan, J.; Shi, K.; Sun, Y.; Wu, Y.; Li, J.; Li, K.; Wu, H.; Wang, Z.; Dong, H.; Liu, Q. Activating redox kinetics of polysulfides within edge-rich nitrogen doped porous interconnected carbon nanosphere. Chem. Eng. Sci. 2023, 274, 118640-118652.

[5] Li, J.; Wang, Z.; Shi, K.; Wu, Y.; Huang, W.; Min, Y.; Liu, Q.; Liang, Z. Nanoreactors Encapsulating Built-in Electric Field as a "Bridge" for Li–S Batteries: Directional Migration and Rapid Conversion of Polysulfides. Adv. Energy Mater. 2023, 14 (9), 2303546-2303558.

[6] Li, T.; Sun, Y.; Shi, K.; Qin, W.; Chen, H.; Li, J.; Zheng, Y.; Liu, Q.; Liang, Z. The d-band energy level splitting of ferric group (Fe, Co, Ni) metals drives the adsorption-conversion of polysulfides. AIChE J. 2023, 70 (3), 1-10.

[7] Fan, Q.; Li, B.; Si, Y.; Fu, Y. Lowering the charge overpotential of Li_2S via the inductive effect of phenyl diselenide in Li–S batteries. Chem Commun. 2019, **55** (53), 7655-7658.

[8] Jiao, L.; Jiang, H.; Lei, Y.; Wu, S.; Gao, Q.; Bu, S.; Kong, X.; Yang, S.; Shu, D.; Li, C.; Li, H.; Cheng, B.; Lee, C.; Zhang, W. "Dual Mediator System" Enables Efficient and Persistent Regulation toward Sulfur Redox Conversion in Lithium–Sulfur Batteries. ACS Nano 2022, 16 (9), 14262-14273.

[9] Feng, T.; Zhao, T.; Zhang, N.; Duan, Y.; Li, L.; Wu, F.; Chen, R. 2D Amorphous Mo-Doped CoB for Bidirectional Sulfur Catalysis in Lithium Sulfur Batteries. Adv. Funct. Mater. 2022, 32 (30), 2202766-2202776.

[10] Sun, W.; Xu, Y.; Chen, X.; Xu, Y.; Wu, F.; Wang, Y. Reduced graphene oxide modified with naphthoquinone for effective immobilization of polysulfides in high-performance Li-S batteries. Chem Eng J. 2020, 383, 1-53.
[11] Zhou, Y.; Zhang, Y.; Li, X. Upcycling of paper waste for high-performance lithium-sulfur batteries. Mater. 2021, 19, 1-37.